Approximate exchange-only entangling gates for the three-spin-1/2 decoherence-free subsystem

James R. van Meter and Emanuel Knill

Phys. Rev. A **99**, 042331 — Published 23 April 2019

DOI: 10.1103/PhysRevA.99.042331

Approximate exchange-only entangling gates for the three-spin-1/2 decoherence-free subsystem

James R. van Meter[1,2] and Emanuel Knill[2,3]

[1] *Department of Mathematics, University of Colorado, Boulder, Colorado 80309, USA*
[2] *National Institute of Standards and Technology, Boulder, Colorado 80305, USA*
[3] *Center for Theory of Quantum Matter, University of Colorado, Boulder, Colorado 80309, USA*

The three-spin-1/2 decoherence-free subsystem defines a logical qubit protected from collective noise and supports exchange-only universal gates. Such logical qubits are well-suited for implementation with electrically-defined quantum dots. Exact exchange-only entangling logical gates exist but are challenging to construct and understand. We use a decoupling strategy to obtain straightforward approximate entangling gates. A benefit of the strategy is that if the physical spins are aligned, then it can implement evolution under entangling Hamiltonians. Hamiltonians expressible as linear combinations of logical Pauli products not involving σ_y can be implemented directly. Self-inverse gates that are constructible from these Hamiltonians, such as the CNOT, can be implemented without the assumption on the physical spins. We compare the control complexity of implementing CNOT to previous methods and find that the complexity for fault-tolerant fidelities is competitive.

I. INTRODUCTION

Three physical spin-1/2 systems support a collective decoherence-free two-level subsystem (the 3DFS) in the four-dimensional subspace with total spin 1/2, where collective noise is induced by global fields acting with total spin operators along any axis. This motivates the use of the 3DFS as a logical qubit [1, 2]. The 3DFS's observables are spanned by the three Hermitian and unitary operators exchanging two of the physical spins, enabling implementation of logical one-qubit gates. These operators are referred to as swaps when used as unitary gates, and as exchange interactions when used as generators of evolution. This definition of the exchange interaction agrees with the conventional one up to a multiple of the identity. We also identify the swap operators with transpositions in the representation of the symmetric group that acts by permuting the physical spins. The best-known application of the 3DFS is to quantum computing with quantum dots where evolution under the exchange interaction can be more accessible than universal one-quantum-dot evolutions [3]. Indeed the requisite control over three quantum dots has been proven feasible by many experimental demonstrations [4–10]. The application to quantum dots is further supported by the ability to implement entangling logical gates between two blocks of physical spins carrying 3DFSs with exchange interactions only [3], but these gates require many steps and are often difficult to construct and understand from first principles (with a possible exception being [11]).

In theory, every logical two-qubit gate is generated by exchange Hamiltonians on the physical spins comprising two 3DFS blocks [12]. In practice constructing such gates is challenging, and constructing them to be independent of the total spin of the two blocks even more so. Since each block has spin 1/2, the total spin of the system is either 0 or 1. While the action on each logical qubit of exchange interactions local to each block is independent of the total spin, the action of cross-block exchange interactions is in general spin-dependent. Thus constructing unitaries from cross-block exchange interactions that act on logical qubits independently of the total spin is nontrivial, but essential for entangling gates that are robust under collective noise on the total system.

Much of the work on exchange-only gates has focused on the CNOT gate. The first exchange-only CNOT gate was found numerically by DiVincenzo et al [3]. It required a total spin of 1 and was only approximate, albeit very accurate. Subsequently, exact CNOT gates from the same sequence of interactions were found in [13] and [14]. A simpler, exact spin-dependent CNOT was later found in [15]. A spin-independent, exchange-only CNOT gate was first published by Fong and Wandzura [16] (although a solution was also claimed, but not given, in [3]). Surprisingly this exact spin-independent solution was simpler, in terms of the number of exchange gates and their analytic coefficients, than that of the original spin-dependent solutions. Since then several other spin-independent, exchange-only CNOT gates have been found [17, 18].

The question then arises of how to compare the efficiencies of these various implementations. They each consist of a product of gates, each of which exponentiates a Hamiltonian that depends linearly on exchange interactions. One measure of complexity, then, is to sum the absolute values of the coefficients on the exchange interactions. Taking the absolute value assumes that the exchange interaction can be turned on with either sign (which is permissible [19–24]). If the exchange interactions are all performed in series, then this measure is proportional to the total evolution time required for the physical operation. Alternatively, if some exchange interactions are performed in parallel, one could instead sum the largest

coefficients for each exponential in the product for the gate, and again this sum is proportional to the total evolution time when operating in parallel mode. By either measure, the Fong and Wandzura construction [16] is one of the most efficient of the exact, exchange-only CNOT gates, and we use it as a benchmark.

We give an alternative approach that constructs approximate entangling logical gates between two 3DFSs. The strategy is to decouple cross-block exchange interactions by within-block operations that project the cross-block interactions into the computational two-qubit subsystem determined by the two 3DFSs. With the orthogonal complement of the computational subsystem thus decoupled, we proceed to construct two-qubit gates from exchange interactions and further show that a large subset of these gates are spin-independent. This task is facilitated by allowing non-commuting exchange interactions to be performed in parallel, as made possible for example by semiconductor quantum dot technology [25]. We then find that for the spin-independent CNOT gate, an entanglement fidelity better than 0.99 can be achieved with a total evolution time that is shorter than that of the exact implementations, and slightly shorter still if spin-dependence is allowed.

This paper is organized as follows. In Section II we review the symmetric group and unitary group representation theory needed to derive our results. In particular, we give explicit maps of the computational subsystems into the symmetric group representations that appear. In Section III we describe our procedure for decoupling the computational subsystem for two 3DFSs from its orthogonal, "leakage" space with exchange interactions. In Section IV we apply this method to construct a spin-independent exchange-only CNOT gate, and spin-dependent exchange-only evolutions optimized for total spin 1. We conclude with a discussion and open problems in Section V.

II. REPRESENTATION THEORY

Here we briefly review the relevant representation theory; for more comprehensive discussion of symmetric group representations see [26], of unitary group representations see [27], and of both applied to quantum information see [28]. The special unitary group of $d \times d$ matrices is denoted by $\mathrm{SU}(d)$, and the symmetric group of permutations of n elements is denoted by S_n, where we are interested in $n = 3$ or $n = 6$. Irreducible representations (irreps) of the groups $\mathrm{SU}(d)$ and S_n are conveniently labeled by partitions of n in a canonical way that is made clear below. For this purpose it is convenient to introduce the notation $\nu \vdash n$ signifying that ν is a partition of n. We also write $|\nu|$ for the size of ν, so $|\nu| = n$, and $\#(\nu)$ for the number of parts of ν. Now we have that for each $\nu \vdash n$ there is an irrep of S_n, which we denote by V_ν, and for each $\nu \vdash n$ such that $\#(\nu) \leq d$ there is an irrep of $SU(d)$, which we denote by U_ν. By convention, each partition can be explicitly denoted by a Young diagram, consisting of a row of cells for each part, arranged in descending order of length, with n cells total. So for $n = 3$ the partitions are

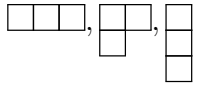

(1)

and therefore the irreps of S_3 are $V_{\square\square\square}$, $V_{\begin{smallmatrix}\square\square\\\square\end{smallmatrix}}$, and $V_{\begin{smallmatrix}\square\\\square\\\square\end{smallmatrix}}$ and the irreps of $SU(2)$ are $U_{\square\square\square}$ and $U_{\begin{smallmatrix}\square\square\\\square\end{smallmatrix}}$.

A convenient choice of basis vectors for each irrep of S_n is labeled by Young tableaux, defined as follows. A Young tableau is a Young diagram in which every cell is filled in with a number from 1 to n, with no repetitions, such that the numbers are increasing along every

row from left to right and along every column from top to bottom. So for the Young diagram $\square\square\square$ the only Young tableau is

$$\ytableaushort{123}, \tag{2}$$

and for the Young diagram $\begin{ytableau}\none&\none\\\none\end{ytableau}$ the Young tableaux are:

$$\ytableaushort{13,2}, \ytableaushort{12,3}. \tag{3}$$

Similarly, a convenient choice of basis vectors for each irrep of $SU(d)$ is labeled by Weyl tableaux (also known as semistandard tableaux), defined as follows. A Weyl tableau is a Young diagram of at most d rows with every cell filled in with a number from 1 to d, with repetitions allowed, such that the numbers are nondecreasing along rows from left to right and increasing along columns from top to bottom. To avoid confusion with the Young tableaux, and because we only consider $d = 2$, we substitute 1 and 2 in Weyl tableaux by an up arrow and a down arrow, respectively. So for the Young diagram $\square\square\square$ the Weyl tableaux are:

$$\ytableaushort{\uparrow\uparrow\uparrow}, \ytableaushort{\uparrow\uparrow\downarrow}, \ytableaushort{\uparrow\downarrow\downarrow}, \ytableaushort{\downarrow\downarrow\downarrow}, \tag{4}$$

corresponding to the four possible spins along the z axis of the spin 3/2 subsystem of three physical spins. For the Young diagram $\begin{ytableau}\none&\none\\\none\end{ytableau}$ the Weyl tableaux are:

$$\ytableaushort{\uparrow\uparrow,\downarrow}, \ytableaushort{\uparrow\downarrow,\downarrow}, \tag{5}$$

corresponding to the two states of the spin 1/2 subsystem of three physical spins.

To complete our specification of each irrep we need to decide on a convention for how each group element is to act on the basis vectors. Our choice for the symmetric group is Young's orthogonal form [29], which is particularly well-suited for quantum mechanical applications because it maps permutations to unitary matrices, and therefore maps transpositions to Hermitian matrices. It is defined on the Young tableau basis as follows. Let T be a Young tableau and for $1 \leq i, j \leq n$ let $d_T(i,j) \equiv (c_T(j) - r_T(j)) - (c_T(i) - r_T(i))$ where $r_T(k)$ and $c_T(k)$ respectively denote the row and column containing number k. Then denoting the transposition in S_n that exchanges i and j by (ij), and its matrix representation on V_λ by $\rho_\lambda((ij))$, we have

$$\rho_\lambda((i\ i+1))T = \frac{1}{d_T(i,i+1)}T + \sqrt{1 - \frac{1}{d_T(i,i+1)^2}}(i\ i+1)T, \tag{6}$$

where $(i\ i+1)T$ denotes direct action on T via exchange of the positions of i and $i+1$. Note that $(i\ i+1)T$ results in an invalid tableau (only) when i and $i+1$ are in the same row or column, but then $d_T(i,i+1) = \pm 1$ and thus the coefficient of the invalid term vanishes. Since transpositions of the form $(i\ i+1)$ generate S_n, the above definition is sufficient to determine the representation of every permutation.

Now consider the Hilbert space $\mathcal{H}$ of three physical spin-1/2 particles. By Schur-Weyl duality [30] there is a vector space isomorphism between $\mathcal{H}$ and $(V_{\square\square\square} \otimes U_{\square\square\square}) \oplus (V_{\begin{ytableau}\none&\none\\\none\end{ytableau}} \otimes U_{\begin{ytableau}\none&\none\\\none\end{ytableau}})$ that commutes with the action of $S_3 \times SU(2)$. Such an isomorphism is called an intertwiner with respect to the group $S_3 \times SU(2)$. We denote the existence of such an intertwiner as

follows:

$$\mathcal{H} \overset{S_3\times SU(2)}{\cong} (V_{\ydiagram{3}} \otimes U_{\ydiagram{3}}) \oplus (V_{\ydiagram{2,1}} \otimes U_{\ydiagram{2,1}}). \tag{7}$$

The Hilbert space on the right-hand side can further be expressed in terms of tableau basis vectors:

$$V_{\ydiagram{3}} \otimes U_{\ydiagram{3}} \cong \text{span}\left\{\begin{array}{|c|c|c|}\hline 1&2&3\\\hline\end{array} \otimes \begin{array}{|c|c|c|}\hline \uparrow&\uparrow&\uparrow\\\hline\end{array}, \begin{array}{|c|c|c|}\hline 1&2&3\\\hline\end{array} \otimes \begin{array}{|c|c|c|}\hline \uparrow&\uparrow&\downarrow\\\hline\end{array}, \begin{array}{|c|c|c|}\hline 1&2&3\\\hline\end{array} \otimes \begin{array}{|c|c|c|}\hline \uparrow&\downarrow&\downarrow\\\hline\end{array}, \begin{array}{|c|c|c|}\hline 1&2&3\\\hline\end{array} \otimes \begin{array}{|c|c|c|}\hline \downarrow&\downarrow&\downarrow\\\hline\end{array}\right\}, \tag{8}$$

$$V_{\ydiagram{2,1}} \otimes U_{\ydiagram{2,1}} \cong \text{span}\left\{\begin{array}{|c|c|}\hline 1&3\\\hline 2\\\cline{1-1}\end{array} \otimes \begin{array}{|c|c|}\hline \uparrow&\uparrow\\\hline \downarrow\\\cline{1-1}\end{array}, \begin{array}{|c|c|}\hline 1&2\\\hline 3\\\cline{1-1}\end{array} \otimes \begin{array}{|c|c|}\hline \uparrow&\uparrow\\\hline \downarrow\\\cline{1-1}\end{array}, \begin{array}{|c|c|}\hline 1&3\\\hline 2\\\cline{1-1}\end{array} \otimes \begin{array}{|c|c|}\hline \uparrow&\downarrow\\\hline \downarrow\\\cline{1-1}\end{array}, \begin{array}{|c|c|}\hline 1&2\\\hline 3\\\cline{1-1}\end{array} \otimes \begin{array}{|c|c|}\hline \uparrow&\downarrow\\\hline \downarrow\\\cline{1-1}\end{array}\right\}. \tag{9}$$

.

The above basis vectors can be related by linear transformation to the conventional product states of the three physical spins, specified in terms of spin basis, by demanding that each swap of the qubits should be consistent with the action of the representation of each transposition on the tableau basis. Here we identify the action of transpositions on the product basis with that of swaps in the obvious way:

$$(ij)\,|b_1\cdots b_i\cdots b_j\cdots b_n\rangle = |b_1\cdots b_j\cdots b_i\cdots b_n\rangle\,. \tag{10}$$

If we further assume the convention that the Weyl tableaux are eigenvectors of the z-component of the spin operator, then up to an overall phase factor we find the following correspondence with the two-qubit 3DFS encoding of [3]:

$$\begin{array}{|c|c|}\hline 1&3\\\hline 2\\\cline{1-1}\end{array} \otimes \begin{array}{|c|c|}\hline \uparrow&\uparrow\\\hline \downarrow\\\cline{1-1}\end{array} \mapsto \quad \tfrac{1}{\sqrt{2}}(|010\rangle - |100\rangle) \quad \equiv |0_L\rangle|\uparrow\rangle \tag{11}$$

$$\begin{array}{|c|c|}\hline 1&3\\\hline 2\\\cline{1-1}\end{array} \otimes \begin{array}{|c|c|}\hline \uparrow&\downarrow\\\hline \downarrow\\\cline{1-1}\end{array} \mapsto \quad \tfrac{1}{\sqrt{2}}(|101\rangle - |011\rangle) \quad \equiv |0_L\rangle|\downarrow\rangle \tag{12}$$

$$\begin{array}{|c|c|}\hline 1&2\\\hline 3\\\cline{1-1}\end{array} \otimes \begin{array}{|c|c|}\hline \uparrow&\uparrow\\\hline \downarrow\\\cline{1-1}\end{array} \mapsto \tfrac{1}{\sqrt{6}}(2|001\rangle - |100\rangle - |010\rangle) \equiv |1_L\rangle|\uparrow\rangle \tag{13}$$

$$\begin{array}{|c|c|}\hline 1&2\\\hline 3\\\cline{1-1}\end{array} \otimes \begin{array}{|c|c|}\hline \uparrow&\downarrow\\\hline \downarrow\\\cline{1-1}\end{array} \mapsto \tfrac{1}{\sqrt{6}}(2|110\rangle - |011\rangle - |101\rangle) \equiv |1_L\rangle|\downarrow\rangle. \tag{14}$$

Therefore the Young tableaux can be identified with logical 0 (0_L) and logical 1 (1_L) as indicated above. It is now clear in terms of representation theory that the independence of this qubit from collective noise on the spin is due to independence from the action of $SU(2)$.

We now consider entangling two such logical qubits. For the goal of constructing gates, we need to calculate the action of cross-block exchange interactions on these qubits. To that end we make use of the following theorem, adapted from [28]:

Theorem 1. *Given irreps V_λ of $S_{|\lambda|}$ and V_μ of $S_{|\mu|}$ and irreps U_λ and U_μ of $SU(d)$,*

$$(V_\lambda \otimes U_\lambda) \otimes (V_\mu \otimes U_\mu) \overset{S_{|\lambda|}\times S_{|\mu|}\times SU(d)}{\cong} \bigoplus_{\substack{\nu\vdash|\lambda|+|\mu|\\ \#(\nu)\le d}} c^\nu_{\mu\lambda} V_\lambda \otimes V_\mu \otimes U_\nu, \tag{15}$$

where the isomorphism is an intertwiner with respect to the indicated group action and $SU(d)$ is assumed to act simultaneously on U_λ and U_μ on the left hand side. Further, the right hand

side is isomorphic to a subspace of the Schur-Weyl sum,

$$\bigoplus_{\substack{\nu\vdash|\lambda|+|\mu|\\ \#(\nu)\leq d}} c^{\nu}_{\mu\lambda} V_\lambda \otimes V_\mu \otimes U_\nu \overset{S_{|\lambda|}\times S_{|\mu|}\times SU(d)}{\hookrightarrow} \bigoplus_{\substack{\nu\vdash|\lambda|+|\mu|\\ \#(\nu)\leq d}} V_\nu \otimes U_\nu, \tag{16}$$

where the inclusion map is a term-by-term intertwiner with respect to the indicated group action such that each Littlewood-Richardson coefficient $c^{\nu}_{\lambda\mu}$ gives the multiplicity of the image of $V_\lambda \otimes V_\mu$ on the left hand side in each corresponding V_ν on the right hand side.

For the case of $\lambda = \mu = \ydiagram{2}$ and $d = 2$, the Littlewood-Richardson coefficients are such that

$$(V_{\ydiagram{2}}\otimes U_{\ydiagram{2}})\otimes(V_{\ydiagram{2}}\otimes U_{\ydiagram{2}}) \cong (V_{\ydiagram{2}}\otimes V_{\ydiagram{2}}\otimes U_{\ydiagram{3}})\oplus(V_{\ydiagram{2}}\otimes V_{\ydiagram{2}}\otimes U_{\ydiagram{2,2}}) \hookrightarrow (V_{\ydiagram{3}}\otimes U_{\ydiagram{3}})\oplus(V_{\ydiagram{2,2}}\otimes U_{\ydiagram{2,2}}) \tag{17}$$

where both maps are intertwiners with respect to $S_3 \times S_3 \times SU(2)$, and term-by-term the inclusion map implies the following two intertwiners:

$$V_{\ydiagram{2}} \otimes V_{\ydiagram{2}} \overset{S_3\times S_3}{\hookrightarrow} V_{\ydiagram{3}} \tag{18}$$

$$V_{\ydiagram{2}} \otimes V_{\ydiagram{2}} \overset{S_3\times S_3}{\hookrightarrow} V_{\ydiagram{2,2}}. \tag{19}$$

The left hand side encodes our two logical qubits, while its four-dimensional image in the five-dimensional $V_{\ydiagram{3}}$ and nine-dimensional $V_{\ydiagram{2,2}}$ is the computational subspace of each. That these intertwiners are with respect to $S_3 \times S_3$ implies that the actions of transpositions local to each block, on the computational subspace, are consistent across irreps. These maps also determine the actions of cross-block transpositions on the computational subspace, albeit in an irrep-dependent manner. This is one of our primary concerns for the remainder of this paper.

Before proceeding it is instructive to consider the $SU(2)$ irreps in order to form a more complete physical interpretation. Observe that the single Weyl basis vector of $U_{\ydiagram{3}}$ is

$$\begin{array}{|c|c|c|}\hline \uparrow & \uparrow & \uparrow \\ \hline \downarrow & \downarrow & \downarrow \\ \hline \end{array}, \tag{20}$$

and the Weyl basis vectors of $U_{\ydiagram{2,2}}$ are

$$\begin{array}{|c|c|c|c|}\hline \uparrow & \uparrow & \downarrow & \downarrow \\ \hline \downarrow & \downarrow \\ \cline{1-2} \end{array}, \quad \begin{array}{|c|c|c|c|}\hline \uparrow & \uparrow & \downarrow & \downarrow \\ \hline \uparrow & \downarrow \\ \cline{1-2} \end{array}, \quad \begin{array}{|c|c|c|c|}\hline \uparrow & \uparrow & \downarrow & \downarrow \\ \hline \uparrow & \uparrow \\ \cline{1-2} \end{array}. \tag{21}$$

By our convention, these basis vectors are eigenvectors of the z component of the total spin operator, with eigenvalues 0 (Eq. (20)), and -1, 0, 1 (Eq. (21)) respectively. Therefore diagram $\ydiagram{3}$ is associated with states of total spin 0 and diagram $\ydiagram{2,2}$ is associated with states of total spin 1.

Returning to symmetric group irreps, and henceforth overloading Young diagrams to denote symmetric group irreps directly, notice that irrep $\ydiagram{3}$ has one extra dimension and irrep $\ydiagram{2,2}$ has five extra dimensions outside of the images of representation $\ydiagram{2} \otimes \ydiagram{2}$ under the intertwiners of Eqs. (18-19). The extra dimension in irrep $\ydiagram{3}$ and one of the extra dimensions in irrep $\ydiagram{2,2}$ each correspond to the image of representation $\ydiagram{3} \otimes \ydiagram{3}$ under the respective intertwiner implied by Theorem 1 for $\lambda = \mu = \ydiagram{3}$, which is associated with states for which each block has total spin 3/2. The four remaining dimensions of irrep $\ydiagram{2,2}$

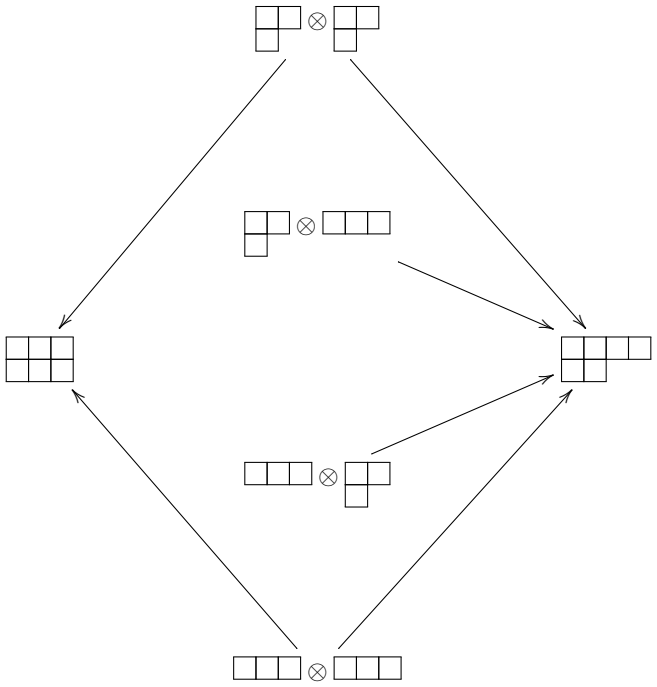

FIG. 1. The injective intertwiners with respect to $S_3 \times S_3$ of the 4-dimensional representation $\ydiagram{2,1} \otimes \ydiagram{2,1}$, the 2-dimensional representation $\ydiagram{2,1} \otimes \ydiagram{3}$, the 2-dimensional representation $\ydiagram{3} \otimes \ydiagram{2,1}$, and the 1-dimensional representation $\ydiagram{3} \otimes \ydiagram{3}$ into the 5-dimesional irrep $\ydiagram{3,3}$ and the 9-dimensional irrep $\ydiagram{3,3,1}$.

correspond to images of representations $\ydiagram{3} \otimes \ydiagram{2,1}$ and $\ydiagram{2,1} \otimes \ydiagram{3}$, which are associated with products of logical qubit states with spin 3/2 states. The multiplicity of each image is one in every case, as determined by the Littlewood-Richardson coefficients, and further clarified by the following vector space isomorphisms:

$$\ydiagram{3,3} \cong \left(\ydiagram{2,1} \otimes \ydiagram{2,1}\right) \oplus \left(\ydiagram{3} \otimes \ydiagram{3}\right) \tag{22}$$

$$\ydiagram{4,2} \cong \left(\ydiagram{2,1} \otimes \ydiagram{2,1}\right) \oplus \left(\ydiagram{2,1} \otimes \ydiagram{3}\right) \oplus \left(\ydiagram{3} \otimes \ydiagram{2,1}\right) \oplus \left(\ydiagram{3} \otimes \ydiagram{3}\right). \tag{23}$$

These various maps are illustrated in Fig. 1.

For the purpose of constructing gates we need to specify the intertwiners $\ydiagram{2,1} \otimes \ydiagram{2,1} \hookrightarrow \ydiagram{3,3}$ and $\ydiagram{2,1} \otimes \ydiagram{2,1} \hookrightarrow \ydiagram{3,3,1}$ explicitly. It suffices to map the Young tableaux basis

$$\left\{ \begin{array}{|c|c|}\hline 1&3\\\hline 2\\\cline{1-1}\end{array} \otimes \begin{array}{|c|c|}\hline 4&6\\\hline 5\\\cline{1-1}\end{array}, \begin{array}{|c|c|}\hline 1&3\\\hline 2\\\cline{1-1}\end{array} \otimes \begin{array}{|c|c|}\hline 4&5\\\hline 6\\\cline{1-1}\end{array}, \begin{array}{|c|c|}\hline 1&2\\\hline 3\\\cline{1-1}\end{array} \otimes \begin{array}{|c|c|}\hline 4&6\\\hline 5\\\cline{1-1}\end{array}, \begin{array}{|c|c|}\hline 1&2\\\hline 3\\\cline{1-1}\end{array} \otimes \begin{array}{|c|c|}\hline 4&5\\\hline 6\\\cline{1-1}\end{array} \right\} \tag{24}$$

of representation $\ydiagram{2,1} \otimes \ydiagram{2,1}$ into irreps $\ydiagram{3,3}$ and $\ydiagram{3,3,1}$. The images of each vector in this basis are determined up to overall phase by demanding that the action of $S_{\{123\}} \times S_{\{456\}}$ on it be consistent with the action of $S_{\{123\}} \times S_{\{456\}}$ on the original basis, where $S_{\{ijk\}}$ denotes

permutations of $\{i, j, k\}$. We then find that for $\ydiagram{2,1} \otimes \ydiagram{2,1} \hookrightarrow \ydiagram{2,2}$,

$$\begin{array}{|c|c|}\hline 1&3\\\hline 2\\\cline{1-1}\end{array} \otimes \begin{array}{|c|c|}\hline 4&6\\\hline 5\\\cline{1-1}\end{array} \mapsto \frac{1}{2}\begin{array}{|c|c|c|}\hline 1&3&5\\\hline 2&4&6\\\cline{1-3}\end{array} - \frac{\sqrt{3}}{2}\begin{array}{|c|c|c|}\hline 1&3&4\\\hline 2&5&6\\\cline{1-3}\end{array}, \tag{25}$$

$$\begin{array}{|c|c|}\hline 1&3\\\hline 2\\\cline{1-1}\end{array} \otimes \begin{array}{|c|c|}\hline 4&5\\\hline 6\\\cline{1-1}\end{array} \mapsto -\frac{\sqrt{3}}{2}\begin{array}{|c|c|c|}\hline 1&3&5\\\hline 2&4&6\\\cline{1-3}\end{array} - \frac{1}{2}\begin{array}{|c|c|c|}\hline 1&3&4\\\hline 2&5&6\\\cline{1-3}\end{array}, \tag{26}$$

$$\begin{array}{|c|c|}\hline 1&2\\\hline 3\\\cline{1-1}\end{array} \otimes \begin{array}{|c|c|}\hline 4&6\\\hline 5\\\cline{1-1}\end{array} \mapsto \frac{1}{2}\begin{array}{|c|c|c|}\hline 1&2&5\\\hline 3&4&6\\\cline{1-3}\end{array} - \frac{\sqrt{3}}{2}\begin{array}{|c|c|c|}\hline 1&2&4\\\hline 3&5&6\\\cline{1-3}\end{array}, \tag{27}$$

$$\begin{array}{|c|c|}\hline 1&2\\\hline 3\\\cline{1-1}\end{array} \otimes \begin{array}{|c|c|}\hline 4&5\\\hline 6\\\cline{1-1}\end{array} \mapsto -\frac{\sqrt{3}}{2}\begin{array}{|c|c|c|}\hline 1&2&5\\\hline 3&4&6\\\cline{1-3}\end{array} - \frac{1}{2}\begin{array}{|c|c|c|}\hline 1&2&4\\\hline 3&5&6\\\cline{1-3}\end{array}, \tag{28}$$

and for $\ydiagram{2,1} \otimes \ydiagram{2,1} \hookrightarrow \ydiagram{3,3}$,

$$\begin{array}{|c|c|}\hline 1&3\\\hline 2\\\cline{1-1}\end{array} \otimes \begin{array}{|c|c|}\hline 4&6\\\hline 5\\\cline{1-1}\end{array} \mapsto \frac{1}{2}\begin{array}{|c|c|c|c|}\hline 1&3&5&6\\\hline 2&4\\\cline{1-2}\end{array} - \frac{\sqrt{3}}{2}\begin{array}{|c|c|c|c|}\hline 1&3&4&6\\\hline 2&5\\\cline{1-2}\end{array}, \tag{29}$$

$$\begin{array}{|c|c|}\hline 1&3\\\hline 2\\\cline{1-1}\end{array} \otimes \begin{array}{|c|c|}\hline 4&5\\\hline 6\\\cline{1-1}\end{array} \mapsto \frac{\sqrt{3}}{6}\begin{array}{|c|c|c|c|}\hline 1&3&5&6\\\hline 2&4\\\cline{1-2}\end{array} + \frac{1}{6}\begin{array}{|c|c|c|c|}\hline 1&3&4&6\\\hline 2&5\\\cline{1-2}\end{array} - \frac{2\sqrt{2}}{3}\begin{array}{|c|c|c|c|}\hline 1&3&4&5\\\hline 2&6\\\cline{1-2}\end{array}, \tag{30}$$

$$\begin{array}{|c|c|}\hline 1&2\\\hline 3\\\cline{1-1}\end{array} \otimes \begin{array}{|c|c|}\hline 4&6\\\hline 5\\\cline{1-1}\end{array} \mapsto \frac{1}{2}\begin{array}{|c|c|c|c|}\hline 1&2&5&6\\\hline 3&4\\\cline{1-2}\end{array} - \frac{\sqrt{3}}{2}\begin{array}{|c|c|c|c|}\hline 1&2&4&6\\\hline 3&5\\\cline{1-2}\end{array}, \tag{31}$$

$$\begin{array}{|c|c|}\hline 1&2\\\hline 3\\\cline{1-1}\end{array} \otimes \begin{array}{|c|c|}\hline 4&5\\\hline 6\\\cline{1-1}\end{array} \mapsto \frac{\sqrt{3}}{6}\begin{array}{|c|c|c|c|}\hline 1&2&5&6\\\hline 3&4\\\cline{1-2}\end{array} + \frac{1}{6}\begin{array}{|c|c|c|c|}\hline 1&2&4&6\\\hline 3&5\\\cline{1-2}\end{array} - \frac{2\sqrt{2}}{3}\begin{array}{|c|c|c|c|}\hline 1&2&4&5\\\hline 3&6\\\cline{1-2}\end{array}. \tag{32}$$

The resulting right hand sides give the computational basis in each irrep. Note the above numbering is consistent with the physical qubit "nearest neighbors" and corresponding product state ordering assumed by DiVincenzo et al. [3, 13].

III. DECOUPLING

Each computational basis defined above spans what we call the computational subspace of each irrep, allowing us to further define the computational submatrix of each matrix representation of a permutation as its projection onto the computational subspace. We find that these computational submatrices of representations of transpositions in irreps $\ydiagram{3,3}$ and $\ydiagram{2,2}$ are rich and varied enough that their linear combinations yield most of the computational Pauli basis. Therefore if we were able to evolve according to projections onto the computational subspace using only exchange interactions, we would have a simple way to construct a wide variety of Hamiltonians and gates. In this section we present just such a method, to good approximation. Our strategy is to remove transitions between the computational subspace and its complement with the general decoupling procedure introduced in [31, 32]. Decoupling involves interspersing pulses with evolution so that the resulting effective Hamiltonian preserves the computational subspace while acting as the projection of the original Hamiltonian on this subspace.

For the purpose of evolving under operators projected onto the computational subspace,

the symmetric sums of local transpositions prove to be useful:

$$\Sigma_a \equiv \frac{1}{3}((12) + (13) + (23)) \tag{33}$$

$$\Sigma_b \equiv \frac{1}{3}((45) + (46) + (56)). \tag{34}$$

It can be easily verified that Σ_a and Σ_b each act as zero on the computational subspace, by accordingly exchanging the physical spins of the product states that constitute the computational basis.

For the sake of consistency with our representation theory approach we introduce the group algebra $\mathbb{C}S_6$, which we have just used implicitly. This consists of all finite linear combinations of S_6,

$$\mathbb{C}S_6 \equiv \{a_1\sigma_1 + \cdots + a_m\sigma_m | a_i \in \mathbb{C}, \sigma_i \in S_6, m \in \mathbb{N}\}, \tag{35}$$

as for example Σ_a and Σ_b. The group algebra comes equipped with multiplication, addition, and scalar multiplication in the obvious ways. It is then straightforward to linearly extend Young's orthogonal representation from S_6 to $\mathbb{C}S_6$, which we assume henceforth. As expected we find $\rho_\lambda(\Sigma_a)$ and $\rho_\lambda(\Sigma_b)$ are each null on the computational subspace.

The sums Σ_a and Σ_b have additional properties that make them well-suited to the task of performing effective projection operations. As they consist of mutually nonoverlapping transpositions, they commute, and therefore their representations can be simultaneously diagonalized. We then have for irrep $\ydiagram{3,3}$,

$$\rho_{\ydiagram{3,3}}(\Sigma_a) = \mathrm{diag}(0,0,0,0,1), \tag{36}$$

$$\rho_{\ydiagram{3,3}}(\Sigma_b) = \mathrm{diag}(0,0,0,0,1), \tag{37}$$

and for irrep $\ydiagram{3,3,2}$,

$$\rho_{\ydiagram{3,3,2}}(\Sigma_a) = \mathrm{diag}(0,0,0,0,1,1,0,0,1), \tag{38}$$

$$\rho_{\ydiagram{3,3,2}}(\Sigma_b) = \mathrm{diag}(0,0,0,0,0,0,1,1,1). \tag{39}$$

where here and henceforth the first four basis vectors of irrep $\ydiagram{3,3}$ are given by the right hand sides of Eqs. (25-28), in that order, the first four basis vectors of irrep $\ydiagram{3,3,2}$ are given by the right hand sides of Eqs. (29-32), in that order (thus corresponding in both cases to the computational basis $\{|00\rangle_L, |01\rangle_L, |10\rangle_L, |11\rangle_L\}$), and the remainder of each basis is such that the following properties hold. The eigenspace of the final 1 in every case is the image of representation $\ydiagram{3} \otimes \ydiagram{3}$, the remaining two-dimensional 1-eigenspace in $\rho_{\ydiagram{3,3,2}}(\Sigma_a)$ is the image of representation $\ydiagram{3}\otimes\ydiagram{2,1}$, and the remaining two-dimensional 1-eigenspace in $\rho_{\ydiagram{3,3,2}}(\Sigma_b)$ is the image of representation $\ydiagram{2,1} \otimes \ydiagram{3}$. So Σ_a and Σ_b can be interpreted as projectors onto states that are disallowed by the computational subspace. Furthermore $\Sigma_a + \Sigma_b \neq 0$ on the complement of the computational subspace in both irreps.

To put these sums to use, we define the following unitaries,

$$U_a \equiv \exp(i\pi\rho_\lambda(\Sigma_a)) \tag{40}$$

$$U_b \equiv \exp(i\pi\rho_\lambda(\Sigma_b)), \tag{41}$$

where λ equals partition $\ydiagram{3,3}$ or $\ydiagram{3,3,2}$. For $\lambda = \ydiagram{3,3}$, and again in the diagonalizing basis

(which includes the computational basis),

$$U_a \equiv \mathrm{diag}(1,1,1,1,-1) \tag{42}$$
$$U_b \equiv \mathrm{diag}(1,1,1,1,-1) \tag{43}$$

and for $\lambda = \ydiagram{4,2}$,

$$U_a \equiv \mathrm{diag}(1,1,1,1,-1,-1,1,1,-1) \tag{44}$$
$$U_b \equiv \mathrm{diag}(1,1,1,1,1,1,-1,-1,-1). \tag{45}$$

It follows that, for all $H \in \rho_\lambda(\mathbb{C}S_6)$ and $\lambda = \ydiagram{3,3}$ or $\ydiagram{4,2}$,

$$\frac{1}{4}(H + U_a H U_a^\dagger + U_b H U_b^\dagger + U_b U_a H U_a^\dagger U_b^\dagger) = D(H), \tag{46}$$

where D denotes a decoupling function which cancels cross terms with the computational subspace. Alternatively we can define

$$U \equiv \exp\left(i\frac{\pi}{2}\rho_\lambda(\Sigma_a + \Sigma_b)\right), \tag{47}$$

and obtain in both irreps,

$$\frac{1}{4}(H + UHU^\dagger + U^\dagger H U + U^2 H (U^2)^\dagger) = D(H), \tag{48}$$

with the choice of unitaries depending on which is more convenient for the problem at hand.

In terms of projection operators,

$$D(H) \equiv \begin{cases} \Pi H \Pi + \Pi_{\ydiagram{3}\otimes\ydiagram{3}} H \Pi_{\ydiagram{3}\otimes\ydiagram{3}}, & H \in \rho_{\ydiagram{3,3}}(\mathbb{C}S_6), \\ \Pi H \Pi + \Pi_{\ydiagram{1}\otimes\ydiagram{3}} H \Pi_{\ydiagram{1}\otimes\ydiagram{3}} + \Pi_{\ydiagram{3}\otimes\ydiagram{1}} H \Pi_{\ydiagram{3}\otimes\ydiagram{1}} + \Pi_{\ydiagram{3}\otimes\ydiagram{3}} H \Pi_{\ydiagram{3}\otimes\ydiagram{3}}, & H \in \rho_{\ydiagram{4,2}}(\mathbb{C}S_6), \end{cases} \tag{49}$$

where Π projects onto the computational subspace while $\Pi_{\ydiagram{1}\otimes\ydiagram{3}}$, $\Pi_{\ydiagram{3}\otimes\ydiagram{1}}$, and $\Pi_{\ydiagram{3}\otimes\ydiagram{3}}$ project onto the subspaces comprising the complement of the computational subspace as indicated in Fig. 1 and Eqs. (22-23). Noting that $\rho_{\ydiagram{3,3}}(\mathbb{C}S_6) \cong M_5(\mathbb{C})$, if we let $H = (h_{ij}) \in \rho_{\ydiagram{3,3}}(\mathbb{C}S_6)$ then we obtain

$$D(H) = \begin{pmatrix} h_{11} & h_{12} & h_{13} & h_{14} & 0 \\ h_{21} & h_{22} & h_{23} & h_{24} & 0 \\ h_{31} & h_{32} & h_{33} & h_{34} & 0 \\ h_{41} & h_{42} & h_{43} & h_{44} & 0 \\ 0 & 0 & 0 & 0 & h_{55} \end{pmatrix}. \tag{50}$$

On the other hand noting that $\rho_{\ydiagram{4,2}}(\mathbb{C}S_6) \cong M_9(\mathbb{C})$, if we let $H = (h_{ij}) \in \rho_{\ydiagram{4,2}}(\mathbb{C}S_6)$ then we

obtain

$$D(H) = \begin{pmatrix} h_{11} & h_{12} & h_{13} & h_{14} & 0 & 0 & 0 & 0 & 0 \\ h_{21} & h_{22} & h_{23} & h_{24} & 0 & 0 & 0 & 0 & 0 \\ h_{31} & h_{32} & h_{33} & h_{34} & 0 & 0 & 0 & 0 & 0 \\ h_{41} & h_{42} & h_{43} & h_{44} & 0 & 0 & 0 & 0 & 0 \\ 0 & 0 & 0 & 0 & h_{55} & h_{56} & 0 & 0 & 0 \\ 0 & 0 & 0 & 0 & h_{65} & h_{66} & 0 & 0 & 0 \\ 0 & 0 & 0 & 0 & 0 & 0 & h_{77} & h_{78} & 0 \\ 0 & 0 & 0 & 0 & 0 & 0 & h_{87} & h_{88} & 0 \\ 0 & 0 & 0 & 0 & 0 & 0 & 0 & 0 & h_{99} \end{pmatrix}. \tag{51}$$

We now recognize projections onto the four-dimensional computational subspace, the two-dimensional subspaces associated with $\square\!\!\square \otimes \square$ and $\square \otimes \square\!\!\square$, and the one-dimensional subspace associated with $\square \otimes \square$, as discussed in Section II.

Our task, then, is to express the above projection procedure in terms of physically-realizable, exchange-only operations. Therefore we "Trotterize", that is approximate

$$\exp(i\alpha D(H)) = \exp\left(i\alpha \left(\frac{1}{4}\sum_{j=1}^{4} U_j H U_j^\dagger\right)\right) \tag{52}$$

as a product of unitaries in the form of exponentials depending on linear combinations of exchange interactions, where α is some angle and $\{U_j\}_{j=1}^4$ is one of $\{1, U_a, U_b, U_a U_b\}$ or $\{1, U, U^\dagger, U^2\}$. Letting $\{A_j\}_{j=1}^k$ be a set of non-commuting operators we can use for example the zeroth order exponential product expansion,

$$\exp\left(\sum_{j=1}^{k} A_j\right) = \left(\prod_{j=1}^{k} \exp\left(\frac{1}{n} A_j\right)\right)^n + O\left(\frac{1}{n}\right), \tag{53}$$

or the first order Suzuki-Trotter expansion [33, 34],

$$\exp\left(\sum_{j=1}^{k} A_j\right) = \left(\prod_{j=2}^{k} \exp\left(\frac{1}{2n} A_{k+2-j}\right) \exp\left(\frac{1}{n} A_1\right) \prod_{j=2}^{k} \exp\left(\frac{1}{2n} A_j\right)\right)^n + O\left(\frac{1}{n^2}\right), \tag{54}$$

or still higher order approximations. Therefore, noting that

$$\exp\Big(i\alpha U_j H U_j^\dagger\Big) = U_j \exp(i\alpha H) U_j^\dagger, \tag{55}$$

and using $\{U_j\}_{j=1}^4 = \{U^2, U, 1, U^\dagger\}$, we have to zeroth order that

$$\exp(i\alpha D(H)) = \Big(U^2 \exp(i\delta t H)(U^2)^\dagger U \exp(i\delta t H) U^\dagger \exp(i\delta t H) U^\dagger \exp(i\delta t H) U\Big)^n + O(\delta t) \tag{56}$$

and to first order that

$$\begin{aligned}\exp(i\alpha D(H)) &= \left(U^\dagger \exp\left(i\frac{\delta t}{2}H\right)U \exp\left(i\frac{\delta t}{2}H\right)U \exp\left(i\frac{\delta t}{2}H\right)U^\dagger U^2 \exp(i\delta t H)(U^2)^\dagger\right. \\ &\quad \left.\times U \exp\left(i\frac{\delta t}{2}H\right)U^\dagger \exp\left(i\frac{\delta t}{2}H\right)U^\dagger \exp\left(i\frac{\delta t}{2}H\right)U\right)^n + O(\delta t^2) \qquad (57) \\ &= U^\dagger \left(\left(\exp\left(i\frac{\delta t}{2}H\right)U\right)^3 \exp(i\delta t H)\left(U^\dagger \exp\left(i\frac{\delta t}{2}H\right)\right)^3\right)^n U + O(\delta t^2).\end{aligned}$$

where $\delta t = \alpha/4n$.

IV. HAMILTONIAN AND GATE CONSTRUCTION

A. One qubit: Spin-independent Hamiltonians and gates

We now explore which combinations of exchange interactions yield useful computational submatrices. First we review the relationship between local exchange interactions and Pauli matrices. The X and Z Pauli matrices on the first qubit can be constructed from any two local exchange interactions within the first block as follows:

$$\begin{aligned}\begin{pmatrix} -\frac{1}{\sqrt{3}} & -\frac{2}{\sqrt{3}} \\ -1 & 0 \end{pmatrix} \Pi\rho_\lambda \begin{pmatrix} (12) \\ (13) \end{pmatrix} \Pi &= \begin{pmatrix} \frac{1}{\sqrt{3}} & \frac{2}{\sqrt{3}} \\ -1 & 0 \end{pmatrix} \Pi\rho_\lambda \begin{pmatrix} (12) \\ (23) \end{pmatrix} \Pi \\ &= \begin{pmatrix} -\frac{1}{\sqrt{3}} & \frac{1}{\sqrt{3}} \\ 1 & 1 \end{pmatrix} \Pi\rho_\lambda \begin{pmatrix} (13) \\ (23) \end{pmatrix} \Pi = \begin{pmatrix} XI \\ ZI \end{pmatrix}, \qquad (58)\end{aligned}$$

where the representation ρ_λ and projector Π are understood to operate on each component of each column vector of transpositions. Thus for example the first row of the left-most term implies

$$-\frac{1}{\sqrt{3}}\Pi\rho_\lambda(12)\Pi - \frac{2}{\sqrt{3}}\Pi\rho_\lambda(13)\Pi = XI \qquad (59)$$

where the projector appears in this equation only for consistency of matrix dimensions across the equal sign (decoupling is not required for single-qubit gates), and by a component of the form AB, where $A, B \in \{I, X, Z\}$, we mean a tensor product of the indicated Pauli matrix on the first qubit with the indicated Pauli matrix on the second qubit. Similarly local exchange interactions within the second block yield Eq. (58) but with (12), (13), and (23) replaced by (45), (46), and (56) respectively, and XI and ZI replaced by IX and IZ respectively.

Now we focus on one of the blocks and so momentarily dispense with tensor products with the identity. We can obtain any Hamiltonian of the form $aX + bZ$ from local exchange interactions, up to phase. A Hamiltonian of the form $aX + bY$ can then be obtained by conjugation with $\exp\left(i\frac{\pi}{4}X\right)$, which transforms Z to Y, and a Hamiltonian of the form $aY+bZ$ can be obtained by conjugation with $\exp\left(i\frac{\pi}{4}Z\right)$, which transforms X to Y.

More generally, for any single-qubit Hamiltonian H and time t it follows from a Cartan

decomposition of $SU(2)$ (a generalized Euler angle decomposition of rotations) [35] that

$$\exp(iHt) = \exp(i\delta I)\exp(i\alpha X)\exp(i\beta Z)\exp(i\gamma X), \tag{60}$$

for some $\alpha, \beta, \gamma, \delta \in \mathbb{R}$, which can then be expressed in terms of local exchange interactions by Eq. (58). Thus we can construct any single-qubit gate from local exchange interactions. Such constructions are independent of the choice of irrep ($\ydiagram{3}$ or $\ydiagram{3,1}$) since the relevant intertwiners preserve the action of local exchange interactions.

B. Two qubits: Spin-dependent Hamiltonians and spin-independent gates

Constructing exchange-only Hamiltonians for two-qubits is more challenging. From calculations performed in Maple 2016 (see Supplemental Material for the Maple-generated files `spin0_exchange_gates` and `spin1_exchange_gates`) we find:

$$\begin{pmatrix} \frac{1}{5} & \frac{1}{5} & \frac{1}{5} & \frac{1}{5} & \frac{1}{5} & \frac{1}{5} & \frac{1}{5} & \frac{1}{5} & \frac{1}{5} \\ -\sqrt{3} & \sqrt{3} & 0 & -\sqrt{3} & \sqrt{3} & 0 & -\sqrt{3} & \sqrt{3} & 0 \\ -1 & -1 & 2 & -1 & -1 & 2 & -1 & -1 & 2 \\ -\sqrt{3} & -\sqrt{3} & -\sqrt{3} & \sqrt{3} & \sqrt{3} & \sqrt{3} & 0 & 0 & 0 \\ -1 & -1 & -1 & -1 & -1 & -1 & 2 & 2 & 2 \\ \frac{3}{2} & -\frac{3}{2} & 0 & -\frac{3}{2} & \frac{3}{2} & 0 & 0 & 0 & 0 \\ \frac{\sqrt{3}}{2} & \frac{\sqrt{3}}{2} & -\sqrt{3} & -\frac{\sqrt{3}}{2} & -\frac{\sqrt{3}}{2} & \sqrt{3} & 0 & 0 & 0 \\ \frac{\sqrt{3}}{2} & -\frac{\sqrt{3}}{2} & 0 & \frac{\sqrt{3}}{2} & -\frac{\sqrt{3}}{2} & 0 & -\sqrt{3} & \sqrt{3} & 0 \\ \frac{1}{2} & \frac{1}{2} & -1 & \frac{1}{2} & \frac{1}{2} & -1 & -1 & -1 & 2 \end{pmatrix} \Pi\rho_\lambda \begin{pmatrix} (14) \\ (15) \\ (16) \\ (24) \\ (25) \\ (26) \\ (34) \\ (35) \\ (36) \end{pmatrix} \Pi = a_\lambda \begin{pmatrix} b_\lambda II \\ IX \\ IZ \\ XI \\ ZI \\ XX \\ XZ \\ ZX \\ ZZ \end{pmatrix}, \tag{61}$$

where $a_\lambda = b_\lambda = 1$ for $\lambda = \ydiagram{3,1}$ and $a_\lambda = -3$ and $b_\lambda = -1/5$ for $\lambda = \ydiagram{3}$. Thus within each irrep we can construct any linear combination of Pauli Hamiltonians excluding Y by decoupling sums of exchange interactions. As before, combinations of X and Y or Z and Y on one qubit can be obtained by appropriate conjugation with $\exp\big(i\frac{\pi}{4}(ZI)\big)$, $\exp\big(i\frac{\pi}{4}(XI)\big)$, $\exp\big(i\frac{\pi}{4}(IZ)\big)$, or $\exp\big(i\frac{\pi}{4}(IX)\big)$.

For any two-qubit gate G it follows from a Cartan decomposition of $SU(4)$ that [35]

$$G = K_1 \exp(i\alpha XX + i\beta YY + i\gamma ZZ)K_2, \tag{62}$$

for some local unitaries K_1 and K_2 and real coefficients α, β, γ. The local unitaries can be expressed in terms of X and Z as discussed previously. The remaining exponential can be further decomposed since XX, YY, and ZZ all commute; for example:

$$\begin{aligned} G &= K_1 \exp(i\alpha XX)\exp(i\beta YY)\exp(i\gamma ZZ)K_2 && (63) \\ &= K_1 \exp(i\alpha XX)\exp\Big(i\frac{\pi}{4}(XI + IX)\Big)\exp(i\beta ZZ) \\ &\quad \times \exp\Big(-i\frac{\pi}{4}(XI + IX)\Big)\exp(i\gamma ZZ)K_2. && (64) \end{aligned}$$

The above Hamiltonian and gate constructions are irrep-dependent, in general. However, consider an exchange-only Hamiltonian H equal to a combination of the above Pauli terms in the $\ydiagram{3,1}$ irrep that squares to the identity. Then using that H equals the same combination of Pauli terms multiplied by -3 in the $\ydiagram{3}$ irrep (neglecting a possible identity term contribution to overall phase) we have by Euler's formula for matrices that $\exp\left(i\frac{\pi}{2}H\right)$ is irrep-independent. For example,

$$\begin{aligned}\exp\left(i\frac{3\pi}{4}\Pi\rho_{\ydiagram{3}}((14)-(15)-(24)+(25))\Pi\right) &= \exp\left(-i\frac{3\pi}{2}XX\right) \\ &= iXX \\ &= \exp\left(i\frac{\pi}{2}XX\right) \\ &= \exp\left(i\frac{3\pi}{4}\Pi\rho_{\ydiagram{2,2}}((14)-(15)-(24)+(25))\Pi\right)\end{aligned} \tag{65}$$

Similarly the general gate G in Eq. (64) is irrep-independent for coefficients $\alpha, \beta, \gamma \in \{-\pi/2, 0, \pi/2\}$. This procedure is used for the CNOT gate in the next section.

C. Spin-independent CNOT

Observe that

$$\frac{1}{2}(IX - ZX) = \begin{pmatrix} 0 & 0 & 0 & 0 \\ 0 & 0 & 0 & 0 \\ 0 & 0 & 0 & 1 \\ 0 & 0 & 1 & 0 \end{pmatrix}. \tag{66}$$

Further, letting

$$N \equiv \frac{3\sqrt{3}}{4}((15)-(14)+(25)-(24)), \tag{67}$$

we immediately obtain from subtraction of the 2nd and 8th rows of Eq. (61) that

$$\Pi\rho_{\ydiagram{2,2}}(N)\Pi = \frac{1}{2}(IX - ZX), \tag{68}$$

and

$$\Pi\rho_{\ydiagram{3}}(N)\Pi = -3\Pi\rho_{\ydiagram{2,2}}(N)\Pi. \tag{69}$$

Clearly then

$$\exp\left(i\frac{\pi}{2}\Pi\rho_{\ydiagram{2,2}}(N)\Pi\right) = \exp\left(i\frac{\pi}{2}\Pi\rho_{\ydiagram{3}}(N)\Pi\right) \tag{70}$$

by the same logic as in the example above (Eq. (66)), albeit with the Hamiltonian $\Pi\rho_{\ydiagram{2,2}}(N)\Pi$ squaring to a two-dimensional rather than four-dimensional identity. Meanwhile $I-(12)$, being local, acts the same on the computational subspace of both irreps:

$$\Pi\frac{1}{2}\rho_{\ydiagram{2,2}}(I-(12))\Pi = \Pi\frac{1}{2}\rho_{\ydiagram{3}}(I-(12))\Pi = \mathrm{diag}(1,1,0,0). \tag{71}$$

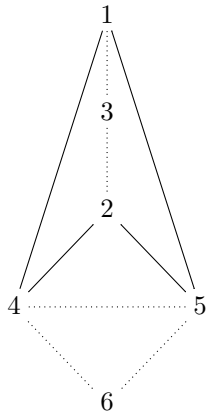

FIG. 2. Qubits arranged so that exchange interactions in the spin-independent CNOT are between neighbors. Solid lines denote exchange interactions in the Hamiltonian yielding the CNOT submatrix while dotted lines denote local interactions used only for the decoupling procedure.

Thus by Eq. (58) the following expression maps to an approximate CNOT on the computational subspace of both irreps,

$$\exp\left(-i\frac{\pi}{4}(I+(12))\right)U^\dagger\left(\left(\exp\left(i\frac{\delta t}{2}N\right)U\right)^3\exp(i\delta tN)\left(U^\dagger\exp\left(i\frac{\delta t}{2}N\right)\right)^3\right)^n U$$
$$=\texttt{CNOT}+O(\delta t^2), \tag{72}$$

where $\delta t=\pi/8n$, and for ease of notation we have dropped the explicit ρ_λ mapping as well as the decoupled orthogonal projection.

Conveniently, the above Hamiltonian and its Trotterization can be recast as neighboring exchange interactions in planar geometry (Fig. 2), where (12) has been removed from U because it commutes with N. (In general if any one local exchange interaction commutes with the Hamiltonian, then since it also commutes with the sum of the remaining local interactions it cancels during conjugation and can thus be removed.) That (12) commutes with N is due to the fact that N is symmetric with respect to qubits 1 and 2 and thus invariant under conjugation with (12). We add that the exact diagram in Fig. 2 may not be physically practical due to the relative distances between qubits 1, 4 and 5, but more practical architectures may be possible.

To evaluate the efficiency of our approximate CNOT we can define a normalized operation time by summing the maximum magnitude of the coefficients on the exchange interactions in each exponential and dividing by $\pi/2$ (the time required for one full swap). This normalized time is proportional to the actual physical time provided the exchange interactions are performed in parallel. Alternatively we can consider the number of clock cycles, as defined in [3], which here equates to the number of exponential factors in Eq. (72) (after consolidating commuting exponents). To assess the quality of our approximate CNOT we can use the entanglement fidelity [36],

$$F(G,\texttt{CNOT})=\left(\frac{1}{4}\mathrm{tr}(\Pi G^\dagger\texttt{CNOT})\right)^2. \tag{73}$$

n	cycles	time	fidelity	leakage
3	39	8.5	0.99136	0.00552
5	63	12.5	0.99888	0.00070
9	111	20.5	0.99989	0.00007

TABLE I. Clock cycles, normalized time (such that one unit equals the duration of one swap), entanglement fidelity (Eq. (73)), and leakage (Eq. (74)) for various iterations n of the spin-independent CNOT approximation given by Eq. (72). The listed values for fidelity and leakage assume a total spin of 1. The values for cycles and time may be compared with that of the fiducial exact solution of [16], with 13 clock cycles and a normalized time of 12.3.

We also calculate the contribution from leakage out of the computational subspace to $1-F$:

$$L(G, \texttt{CNOT}) = \frac{1}{4}\mathrm{tr}(\Pi G^\dagger \texttt{CNOT} \Pi^\perp \texttt{CNOT}^\dagger G), \tag{74}$$

where G is the gate under consideration and CNOT has been extended by identity to the complement of the computational subspace. Then for various iterations n of the approximation above we obtain the values in Table I, where the fidelity and leakage values assume a total spin of 1, this being the worst case (heuristically because its higher dimensional subsystem has more cross-terms to decouple). If negative exchange interactions are canceled in the optimal way described in Section V, the normalized time is increased by 1.3 in every case but the fidelities and leakages are unchanged. The above times are comparable to that of one of the most efficient exact solutions [16], which has a normalized time of 12.3 (including the local unitaries required for consistency with our computational basis) or 14.8 if negative exchange interactions are canceled.

D. Spin 1 optimized CNOT

Alternatively the qubits can be prepared with a total spin of 1 by the use of magnetic fields [3], in which case spin-independence is not a concern, and the IX term in the above derivation of CNOT can be expressed in terms of local interactions instead of cross-block interactions. In combination with the noncommuting cross-block interactions in the ZX term, this replacement breaks irrep-independence, since the two kinds of interactions transform differently across irreps. However the resulting approximation is made slightly more efficient, as we show below.

Let

$$N_1 \equiv \frac{\sqrt{3}}{4}((56) - (46) + 3((34) - (35))). \tag{75}$$

Then for spin 1 we have

$$\Pi \rho_{\square\square}(N_1)\Pi = \texttt{CNOT}. \tag{76}$$

Unlike the previous spin-independent expression, N_1 commutes with $U_b N_1 U_b^\dagger$ and similarly $U_a N_1 U_a^\dagger$ commutes with $U_a U_b N_1 U_b^\dagger U_a^\dagger$. This simplifies the Suzuki-Trotter approximation for

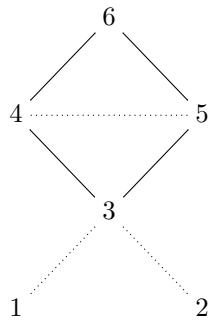

FIG. 3. Qubits arranged so that exchange interactions in the spin-dependent CNOT are between neighbors. Solid lines denote exchange interactions in the Hamiltonian yielding the CNOT submatrix while dotted lines denote local interactions used only for the decoupling procedure.

n	cycles	time	fidelity	leakage
2	21	9.8	0.99849	0.00067
3	31	13.8	0.99970	0.00014
4	41	17.8	0.99990	0.00004

TABLE II. Clock cycles, normalized time (such that one unit equals the duration of one swap), entanglement fidelity (Eq. (73)), and leakage (Eq. (74)) for various iterations n of the spin 1 CNOT approximation given by Eq. (77). The above values for cycles and time may be compared with that of the fiducial exact solution of [16], with 13 clock cycles and a normalized time of 12.3.

$\exp\Big(i\alpha(N_1 + U_a N_1 U_a^\dagger + U_b N_1 U_b^\dagger + U_b U_a N_1 U_a^\dagger U_b^\dagger)\Big)$ and we find

$$\exp\left(-i\frac{\pi}{4}(I + (12))\right)(T^{1/2}U_a T^{1/2}U_a^\dagger U_b T U_a T U_b^\dagger T^{1/2}U_a^\dagger T^{1/2})^n = \texttt{CNOT} + O(\delta t^2), \qquad (77)$$

where $T \equiv \exp(i\delta t N_1)$ and $\delta t = \pi/8n$. Again this can be arranged as neighboring exchange interactions in a plane (Fig. 3), where (12) commutes with N_1 and so can be removed from U_a.

The smaller truncation error that results from this expression yields the results shown in Table II. Again if subtracted exchange interactions are canceled the normalized time is increased by 1.3 in every case.

V. DISCUSSION

For the case of two logical qubits encoded on a decoherence-free subsystem of three physical spins each, we have presented an exchange-only method to decouple the resulting computational subspace from leaked states. Using Trotterization we showed how this method can be implemented to any desired fidelity. We then applied this procedure to explicitly construct Pauli Hamiltonians from exchange interactions. Building on this we provided a transparent method to construct two-qubit gates from exchange interactions, including a

large family of spin-independent gates. In particular we have shown that an exchange-only CNOT gate can be implemented with a computational speed comparable to or better than previous solutions, with good fidelity, provided the exchange interactions can be performed in parallel. The fidelities for these constructions exceed 0.99, which is comparable to fidelities demonstrated for one logical qubit in three quantum dots [10], and for two-qubit gates with other quantum devices [37–39]. Fidelities exceeding the conservative requirements for fault-tolerance [40–42] can be achieved with a slow down of about a factor of two.

We note that for quantum dots the negative coefficients on exchange interactions in many of the expressions above would seem to require negative charging energies [43]. This is possible by coupling to magnetic fields or other means [19–24], but if it proves impractical, the negative coefficients can be removed by various methods. Of course for an exponential of a single negative exchange interaction one may simply add an integer multiple of 2π to its coefficient.

To address the more general case of multiple negative exchange interactions, we observe that the sum of all transpositions in S_6 acts as a constant on the irreps,

$$\rho_\lambda \left(\sum_{j \neq k=1}^{6} (jk) \right) = c_\lambda I, \tag{78}$$

where $c_{\ydiagram{3,3}} = 3$ and $c_{\ydiagram{4,2}} = 5$. Therefore adding the sum of all exchange interactions to an exchange-only Hamiltonian, with a coefficient equal to the largest magnitude of the negative coefficients in that Hamiltonian, will cancel that negative coefficient and ensure that all other resulting coefficients are nonnegative. In general this results in an overall phase difference between the spin 0 and spin 1 cases, due to the different constants effectively being added, but our encoding is independent of such a phase. Alternatively for negative local exchange interactions we can add an appropriate multiple of the sum of all local exchange interactions, for one or both blocks as needed, as that sum acts as zero on the computational subspace (Eqs. (36-39)). It follows that for negative cross-block interactions we can add an appropriate multiple of the sum of all cross-block interactions, as that sum acts as $3I$ or $5I$ on the computational subspace depending again on whether the total spin is 0 or 1. To summarize in more physical terms, the sums discussed above commute with the logical two-qubit observables, which are in the group algebra generated by $S_3 \times S_3$, and can therefore be added to the Hamiltonian as needed without changing relevant expectation values.

We end with some open questions for future work. Aside from the Pauli and CNOT gates, it may be of interest to find efficient expressions for other gates and evaluate their efficiencies as we did for CNOT. Regarding CNOT, we sought to minimize the time required for given fidelities, but one might instead seek to minimize the clock cycles or circuit depth. Related to this, it may be of practical interest to approximate our parallel interaction expressions by strictly serial expressions. Finally, our decoupling procedure employed a first order Suzuki-Trotter approximation, which is optimal for the fidelities considered here, but higher order approximations might be advantageous if higher fidelities are desired. Although the first order approximation can achieve any fidelity with sufficiently many iterations, the higher order approximations require fewer iterations and for large enough fidelity they are more efficient.

ACKNOWLEDGMENTS

JRvM wishes to thank M. Ly, K. Mayer, and N. Thiem for helpful discussions. This work includes contributions of the National Institute of Standards and Technology, which are not subject to U.S. copyright. The identification of any product or trade names is for informational purposes and does not imply endorsement or recommendation by the National Institute of Standards and Technology. This work was performed under the financial assistance award 70NANB18H006 from U.S. Department of Commerce, National Institute of Standards and Technology. JRvM also acknowledges the support of the Professional Research Experience Program at the National Institute of Standards and Technology.

---

[1] P. Zanardi. Stabilizing quantum information. *Phys. Rev. A*, 63:012301/1–, 1999.

[2] E. Knill, R. Laflamme, and L. Viola. Theory of quantum error correction for general noise. *Phys. Rev. Lett.*, 84:2525–2528, 2000.

[3] D. P. DiVincenzo, D. Bacon, J. Kempe, G. Burkard, and K. B. Whaley. Universal quantum computation with the exchange interaction. *Nature*, 408:339–342, 2000. quant-ph/0005116.

[4] E. A. Laird, J. M. Taylor, D. P. DiVincenzo, C. M. Marcus, M. P. Hanson, and A. C. Gossard. Coherent spin manipulation in an exchange-only qubit. *Phys. Rev. B*, 82:075403, Aug 2010.

[5] L. Gaudreau, G. Granger, A. Kam, G. C. Aers, S. A. Studenikin, P. Zawadzki, M. Pioro-Ladrière, Z. R. Wasilewski, and A. S. Sachrajda. Coherent control of three-spin states in a triple quantum dot. *Nature Physics*, 8:54 EP –, 11 2011.

[6] Chang-Yu Hsieh, Yun-Pil Shim, Marek Korkusinski, and Pawel Hawrylak. Physics of lateral triple quantum-dot molecules with controlled electron numbers. *Reports on Progress in Physics*, 75(11):114501, oct 2012.

[7] J. Medford, J. Beil, J. M. Taylor, S. D. Bartlett, A. C. Doherty, E. I. Rashba, D. P. DiVincenzo, H. Lu, A. C. Gossard, and C. M. Marcus. Self-consistent measurement and state tomography of an exchange-only spin qubit. *Nature Nanotechnology*, 8:654 EP –, 09 2013.

[8] Kevin Eng, Thaddeus D. Ladd, Aaron Smith, Matthew G. Borselli, Andrey A. Kiselev, Bryan H. Fong, Kevin S. Holabird, Thomas M. Hazard, Biqin Huang, Peter W. Deelman, Ivan Milosavljevic, Adele E. Schmitz, Richard S. Ross, Mark F. Gyure, and Andrew T. Hunter. Isotopically enhanced triple-quantum-dot qubit. *Science Advances*, 1(4), 2015.

[9] Maximilian Russ and Guido Burkard. Three-electron spin qubits. *Journal of Physics: Condensed Matter*, 29(39):393001, aug 2017.

[10] R. W. Andrews, C. Jones, M. D. Reed, A. M. Jones, S. D. Ha, M. P. Jura, J. Kerckhoff, M. Levendorf, S. Meenehan, S. T. Merkel, A. Smith, B. Sun, A. J. Weinstein, M. T. Rakher, T. D. Ladd, and M. G. Borselli. Quantifying error and leakage in an encoded Si/SiGe triple-dot qubit. *arXiv e-prints*, page arXiv:1812.02693, December 2018.

[11] Daniel Zeuch and N. E. Bonesteel. Simple derivation of the fong-wandzura pulse sequence. *Phys. Rev. A*, 93:010303, Jan 2016.

[12] J. Kempe, D. Bacon, D. A. Lidar, and K. B. Whaley. Theory of decoherence-free fault-tolerant universal quantum computation. *Phys. Rev. A*, 63(4):042307, April 2001.

[13] M. Hsieh, J. Kempe, S. Myrgren, and K. B. Whaley. An explicit universal gate-set for exchange-only quantum computation. *Quantum Information Processing*, 2(4):289–307, August 2003.

[14] Y. Kawano, K. Kimura, H. Sekigawa, M. Noro, K. Shirayanagi, M. Kitagawa, and M. Ozawa. Existence of the exact CNOT on a quantum computer with the exchange interaction. *Quantum Information Processing*, 4(2):65–85, Jun 2005.

[15] Z. Shi, C. B. Simmons, J. R. Prance, J. K. Gamble, T. S. Koh, Y.-P. Shim, X. Hu, D. E. Savage, M. G. Lagally, M. A. Eriksson, M. Friesen, and S. N. Coppersmith. Fast hybrid silicon double-quantum-dot qubit. *Physical Review Letters*, 108(14):140503, April 2012.

[16] Bryan H. Fong and Stephen M. Wandzura. Universal quantum computation and leakage reduction in the 3-qubit decoherence free subsystem. *Quantum Information & Computation*, 11(11-12):1003–1018, 2011.

[17] F. Setiawan, H.-Y. Hui, J. P. Kestner, X. Wang, and S. D. Sarma. Robust two-qubit gates for exchange-coupled qubits. *Phys. Rev. B*, 89(8):085314, February 2014.

[18] D. Zeuch, R. Cipri, and N. E. Bonesteel. Analytic pulse-sequence construction for exchange-only quantum computation. *Phys. Rev. B*, 90(4):045306, July 2014.

[19] Guido Burkard, Daniel Loss, and David P. DiVincenzo. Coupled quantum dots as quantum gates. *Phys. Rev. B*, 59:2070–2078, Jan 1999.

[20] N.T. Bagraev, A.D. Bouravleuv, L.E. Klyachkin, A.M. Malyarenko, and I.A. Shelykh. Negative-U properties for a quantum dot. *Physica B: Condensed Matter*, 340-342:1061 – 1064, 2003. Proceedings of the 22nd International Conference on Defects in Semiconductors.

[21] C. Holmqvist, D. Feinberg, and A. Zazunov. Emergence of a negative charging energy in a metallic dot capacitively coupled to a superconducting island. *Phys. Rev. B*, 77(5):054517, February 2008.

[22] T. Ojanen, F. C. Gethmann, and F. von Oppen. Electromechanical instability in vibrating quantum dots with effectively negative charging energy. *Phys. Rev. B*, 80(19):195103, November 2009.

[23] T.-F. Fang, S.-F. Zhang, C.-J. Niu, and Q.-f. Sun. Bipolaronic blockade effect in quantum dots with negative charging energy. *EPL (Europhysics Letters)*, 105:47006, February 2014.

[24] Guenevere E.D.K. Prawiroatmodjo, Martin Leijnse, Felix Trier, Yunzhong Chen, Dennis V. Christensen, Merlin Von Soosten, Nini Pryds, and Thomas S. Jespersen. Transport and excitations in a negative-U quantum dot at the LaAlO3/SrTiO3 interface. *Nature Communications*, 8(1), 12 2017.

[25] Yun-Pil Shim and Charles Tahan. Charge-noise-insensitive gate operations for always-on, exchange-only qubits. *Phys. Rev. B*, 93:121410, Mar 2016.

[26] W. Fulton, W.F.J. Harris, and J. Harris. *Representation Theory: A First Course*. Graduate Texts in Mathematics. Springer New York, 1991.

[27] J.D. Louck. *Unitary Symmetry and Combinatorics*. World Scientific Publishing Company, 2008.

[28] A. W. Harrow. Applications of coherent classical communication and the Schur transform to quantum information theory. *eprint arXiv:quant-ph/0512255*, December 2005.

[29] A. Young. *The collected papers of Alfred Young 1873-1940*. Mathematical expositions. University of Toronto Press, 1977.

[30] Hermann Weyl. *The Classical Groups: Their Invariants and Representations*. Princeton University Press, 1966.

[31] L. Viola, E. Knill, and S. Lloyd. Dynamical decoupling of open quantum systems. *Physical Review Letters*, 82:2417–2421, March 1999.

[32] L. Viola, S. Lloyd, and E. Knill. Universal control of decoupled quantum systems. *Physical Review Letters*, 83:4888–4891, December 1999.

[33] H. F. Trotter. On the product of semi-groups of operators. *Proceedings of the American Mathematical Society*, 10(4):545–551, 1959.

[34] Masuo Suzuki. Generalized Trotter's formula and systematic approximants of exponential operators and inner derivations with applications to many-body problems. *Comm. Math. Phys.*, 51(2):183–190, 1976.

[35] Navin Khaneja and Steffen J. Glaser. Cartan decomposition of SU(2n) and control of spin systems. *Chemical Physics*, 267(1):11 – 23, 2001.

[36] M. A. Nielsen. The Entanglement fidelity and quantum error correction. 1996.

[37] R. Barends, J. Kelly, A. Megrant, A. Veitia, D. Sank, E. Jeffrey, T. C. White, J. Mutus, A. G. Fowler, B. Campbell, Y. Chen, Z. Chen, B. Chiaro, A. Dunsworth, C. Neill, P. O'Malley, P. Roushan, A. Vainsencher, J. Wenner, A. N. Korotkov, A. N. Cleland, and J. M. Martinis. Superconducting quantum circuits at the surface code threshold for fault tolerance. *Nature (London)*, 508:500–503, April 2014.

[38] J. P. Gaebler, T. R. Tan, Y. Lin, Y. Wan, R. Bowler, A. C. Keith, S. Glancy, K. Coakley, E. Knill, D. Leibfried, and D. J. Wineland. High-fidelity universal gate set for $^{9}\mathrm{be}^{+}$ ion qubits. 117:060505, 2016.

[39] C. J. Ballance, T. P. Harty, N. M. Linke, M. A. Sepiol, and D. M. Lucas. High-fidelity quantum logic gates using trapped-ion hyperfine qubits. *Phys. Rev. Lett.*, 117:060504, Aug 2016.

[40] John Preskill. Reliable quantum computers. *Proc. Roy. Soc. Lond.*, A454:385–410, 1998.

[41] E. Knill. Physics: Quantum computing. *Nature (London)*, 463:441–443, January 2010.

[42] T. D. Ladd, F. Jelezko, R. Laflamme, Y. Nakamura, C. Monroe, and J. L. O'Brien. Quantum computers. *Nature (London)*, 464:45–53, March 2010.

[43] Daniel Loss and David P. DiVincenzo. Quantum computation with quantum dots. *Phys. Rev. A*, 57:120–126, Jan 1998.